Dosimetric Effect of Respiratory Motion On Planned Dose In Whole-Breast Volumetric Modulated Arc Therapy Using Standard And Ultra-Hypofractionation

Mikko Mankinen (mankinen.mikko@gmail.com)
Central Finland Hospital Nova https://orcid.org/0000-0002-2266-1438
Tuomas Virén
Kuopio University Hospital (KUH)
Jan Seppälä
Kuopio University Hospital (KUH)
Heikki Hakkarainen
Central Finland Hospital Nova
Tuomas Koivumäki
Central Finland Hospital Nova

Research

Keywords: breast cancer, whole-breast irradiation, volumetric modulated arc therapy, respiratory motion, ultra-hypofractionation

Posted Date: October 6th, 2021

DOI: https://doi.org/10.21203/rs.3.rs-951443/v1

Version of Record: A version of this preprint was published at Radiation Oncology on March 5th, 2022. See the published version at https://doi.org/10.1186/s13014-022-02014-5.

Abstract

Background and purpose: The interplay effects of respiratory motion and MLC movement on the planned dose in right-sided whole-breast irradiation (WBI) were studied by simulating hypofractionated VMAT treatment courses.

Materials and methods: Ten patients with phase-triggered 4D-CT images were included in the study. VMAT plans targeting the right breast were created retrospectively with prescription doses of 26 Gy (5 fractions) and 40.05 Gy (15 fractions). 3D-CRT plans were generated as a reference. All plans were divided into respiratory phase-specific plans in fraction-by-fraction basis. The phase-specific dose distributions were deformed and superimposed onto the planning image, forming the course-specific, respiratory motion perturbed dose distribution. Distributions were compared with the original plans and changes due to respiratory motion and choice of fractionation were evaluated.

Results: The respiratory motion perturbed PTV coverage (V95%) decreased by 1.7% and the homogeneity index increased by 0.02 for VMAT techniques, compared to the planned values. Highest decrease in CTV coverage was 0.7%. The largest dose differences were located in the areas of steep dose gradients parallel to respiratory motion. The largest difference in DVH parameters between fractionation schemes was 0.4% of the prescribed dose. Clinically relevant changes to the doses of organs at risk were not observed.

Conclusion: The VMAT techniques were found feasible for WBI with 5 and 15-fraction treatments in terms of respiratory motion induced error. The CTV dose coverage was retained despite the decrease in PTV coverage. No clinical significance was found due to the choice of fractionation.

Introduction

Right-sided breast cancer has traditionally been treated under free-breathing (FB) conditions using tangential fields. Hypofractionation has shortened the breast cancer treatment courses from 25 fractions to 15 fractions [1] an even 5-fraction treatment course is gradually gaining acceptance [2,3]. Hypofractionation will reduce costs and time required in breast cancer treatment [4]. However, the new emerging fractionation schemes have increased the plan quality requirements which are not always achievable with conventional treatment techniques. The Volumetric modulated arc therapy (VMAT) technique has been utilized in treating breast cancer, as it has been proven to yield high coverage and improved homogeneity on the target dose [5-7]. However, possible errors caused by the interplay effects of respiratory motion and multi-leaf collimator (MLC) movement of highly modulated fields have raised a concern.

The effects of respiratory motion have been studied for tangential treatment techniques [8-11], but the feasibility of VMAT techniques has not been investigated for whole-breast irradiation (WBI) under free-breathing conditions. Previously, the effects of breathing motion on WBI dose distribution have been simulated using isocenter shifts and weighted end-expiration and end-inspiration dose calculations [8-10]. However, incorporating a realistic respiratory cycle is challenging and only two studies using a four-dimensional computed tomography (4D-CT) image set and IMRT technique to investigate the effect of breathing motion on breast irradiation has been published [11,12]. In addition, the dose averaging effect in 5-fraction WBI under FB conditions is yet to be studied.

This study is the first to evaluate the feasibility of VMAT technique in right-sided WBI under free-breathing conditions by simulating the delivered dose on 4D-CT image sets. In addition, the differences in dose averaging effects between standard hypofractionation (15 fr) and ultra-hypofractionation (5 fr) are evaluated.

Materials And Methods

Ten patients originally diagnosed with lung cancer with 4D-CT images were included in this study. The whole-breast target volumes were delineated according to the ESTRO guideline [13]. As acceptance criteria, a real-time position management (RPM, Varian Medical Systems, Palo Alto, CA) dataset and fully imaged breast region with at least 2 cm margins both cranially and caudally were required. The study protocol was approved by Central Finland Health Care District.

Ten phase-triggered 4D-CT images per patient were acquired using Siemens mCT (Siemens Healthcare GmbH, Erlangen, Germany) with 2 mm slice thickness. Patients were instructed to breathe calmly and were imaged in a supine position. End-inspiration and end-

expiration phase markers were placed automatically in the RPM data and corrected by a radiotherapist if necessary.

The clinical target volume (CTV) was delineated on the end-inspiration image by an oncologist and expanded by 5 mm to form the planning target volume (PTV). The PTV and CTV structures were cropped 5 mm inside from the skin to form PTVin and CTVin. In addition, the PTV was expanded 8 mm outside the body to be used in conjunction with a virtual bolus [14].

The organs-at-risk (OAR) were automatically delineated using MIM Maestro software (MIM Software Inc, Cleveland, OH) based on national atlas for breast cancer [15], and verified by the planning physicist. The delineated OAR structures were lungs, heart, contralateral breast and liver.

A representative respiratory cycle was formed for each patient by averaging the RPM respiratory cycles. The average cycles were sampled to the median prefiltered respiratory cycle length for each patient. In addition, the range of chest wall movement perpendicular to the planned tangential field central axis was determined for each patient. The midpoint slice of CTV, in cranial-caudal direction, was chosen as the measurement location.

VMAT plans were generated using Varian Rapid Arc and Elekta VMAT (RA and E-VMAT). Three-dimensional conformal radiation therapy (3D-CRT) treatment plans with tangential main fields and 2-3 subfields were generated for reference. 3D-CRT and RA plans were created using the Eclipse (Varian Medical Systems) treatment planning system (TPS) with the Photon Optimizer planning algorithm and analytical anisotropic algorithm (AAA) 15.6 for dose calculation. E-VMAT plans were created in Monaco TPS (Elekta AB, Stockholm, Sweden) and dose was calculated using the X-ray Voxel Monte Carlo algorithm. The planning was conducted on 15-fraction plans and the 5-fraction plans were formed by adjusting the fraction count and prescribed dose. The treatment plans were normalized to the mean dose of PTVin. Dose rate was limited to 600 MU/min.

An 11 mm virtual bolus was utilized in RA and E-VMAT treatment planning. The VMAT fields were restricted to tangential directions [7]. Posterior arcs ranged between 181 and 260-275° and the anterior arcs between 325-360° and 60-70° according to individual patient anatomy. The collimator angles for posterior and anterior arc fields were ±5-20° for RA and ±2° E-VMAT. The planning goal was that 95% of the prescribed dose covered 95% of the PTVin and 98% of the CTVin. The V107% was limited to 1 cc. The mean dose of ipsilateral lung was limited to 20% of the prescribed dose. In addition, the volume of 16 Gy dose was limited to 20% of the ipsilateral lung. Similarly, mean doses to contralateral lung, breast and heart were limited to 1 Gy. In addition, the normal tissue V110% was limited to 1cc.

A custom-made Matlab script (2020b, MathWorks Inc, MA) was used to divide the plans into respiratory phase-specific subplans, where the dose rate was zeroed between control points (CP) not coinciding with chosen respiratory phase. For VMAT plans, the starting respiratory phases for the first anterior and posterior arcs were randomly determined for each fraction (Figure 1). The starting phases of the second anterior and posterior fields were subsequent to the last phase of the preceding arc. The gantry angles coinciding with the respiratory phases were solved using the representative respiratory cycle and gantry rotation speed. CPs were added to the plans with a tolerance of ±0.1°, if the respiratory phase changed between the original CPs.

Similarly, the starting respiratory phases of anterior and posterior 3D-CRT fields were determined randomly, and the plans were divided into phase-specific subplans, according to the amount of monitor units (MU) per field. Average pauses between fields, 2.1 seconds after the open field and 1.1 seconds between subfields, were adapted into the division algorithm.

The dose calculations and deformations were performed using MIM Maestro software with SureCalc Monte Carlo dose calculation algorithm and generic beam models for Varian Truebeam and Elekta Infinity linear accelerators. The phase-specific plans were calculated in the corresponding respiratory phase image, and deformed and superimposed onto the end-inspiration phase planning image, creating a fraction-specific dose distribution. All the fraction-specific dose distributions were summed to form the final course-specific distribution per technique and fractionation scheme. A total of 6 simulated course-specific dose distributions were accumulated per patient. Finally, the original treatment plans were calculated using the generic beam models in MIM and differential dose distributions were formed by subtracting the planned dose from the simulated dose.

Dose volume histograms (DVH) were compared between the original and simulated distributions for both fractionations. In addition to the planning objectives, the maximum dose to 1 cc volume (D1cc) was evaluated for all structures. The minimum dose to 1 cc (Min%), conformity index (CI) and homogeneity index (HI) were evaluated for PTVin and CTVin. HI and CI were calculated using

formulas (D2% - D98%) / $D_{prescription}$ and $V95\%_{total}$ / $V_{structure}$, respectively. The statistical difference between the DVH parameters was determined by Wilcoxon signed rank test ($p<0.05$).

The differential distributions were deformed to an anatomy of one patient to localize the statistically significant differences between original and simulated dose. Student's t-test was performed on the differential distributions on a voxel-by-voxel basis including adjacent neighboring voxels. The significance level was adjusted using Benjamini-Hochberg method [16].

Results

The average range of chest wall movement between end-inspiration and end-expiration phases, perpendicular to the 3D-CRT central axis, was 2.4 ± 1.4 mm (range 1.0 – 5.3 mm). The movement exceeded the 5 mm PTV margin for one patient. The median respiratory periods ranged from 2.6 to 6.1 seconds, with 14 to 44 accepted cycles across all patients. The beam-on times of a single fraction were longer for 5-fraction plans. For example, the average beam-on times of 5 and 15-fraction RA plans were 136 seconds (range 121-148 s) and 83 seconds (range 77-93 s), respectively.

Respiratory motion induced a slight decrease in the PTVin coverage for RA (1.4%, $p<0.01$) and E-VMAT (approximately 1.8%, $p<0.01$), respectively (Table 1). Furthermore, a slight decrease in CTVin coverage was found for E-VMAT (approximately 0.5%, $p<0.01$). The PTVin coverage was best retained by the 3D-CRT technique, for which the 5 and 15-fraction dose coverages decreased only by 0.4% ($p=0.262$) and 0.5% ($p=0.052$), respectively. The simulated PTVin coverage decreased below the planning goal in one, two and four plans for 3D-CRT, RA and E-VMAT, respectively. CTVin coverage decreased below 98% in one 3D-CRT plan. Typically, the coverage decreased in the upper and lower medial parts of the PTV or lateral chest wall region. (Figure 2).

The HI of PTVin increased with both VMAT techniques ($p<0.01$) while no significant change was observed with 3D-CRT (Table 1). Furthermore, the HI of CTVin decreased only slightly with 3D-CRT and RA ($p<0.05$), but on the contrary, a greater increase was observed for E-VMAT. The CI of PTVin and CTVin decreased by 0.05 to 0.07 ($p<0.01$) for all techniques.

The maximum dose to 1 cc volume in PTVin decreased for 3D-CRT (108.1 to 107.5%, $p<0.01$) and remained unchanged for RA and E-VMAT. The minimum dose to the 1cc volume (Min1cc) in PTVin decreased for all techniques (Table 1).

The D1cc doses of ipsilateral lung and contralateral breast decreased for almost all techniques (Table 2). Small increases in mean doses were observed for contralateral breast, contralateral lung and heart for E-VMAT ($p<0.01$). Large variation in liver maximum dose was observed (Table 2).

Table 1 legend: Average DVH results for PTVin and CTVin. The Plan and Sim columns indicate the planned and 4D simulated parameters, respectively. The units of V95, D1cc and Min% are presented as percentages of the prescribed dose. Statistical significance between the planned and the simulated dose is represented by bolding ($p<0.05$).

			3D-CRT			RA			E-VMAT	
		Plan	Sim		Plan	Sim		Plan	Sim	
			5fr	15fr		5fr	15fr		5fr	15fr
PTVin	V95%	97.6 ± 1.5	97.2 ± 1.4	97.1 ± 1.3	98.0 ± 0.5	**96.6 ± 1.3**	**96.6 ± 1.2**	97.6 ± 0.9	**95.9 ± 1.1**	**95.8 ± 1.1**
	D1cc	108.1 ± 1.0	**107.5 ± 0.9**	**107.5 ± 1.1**	106.2 ± 0.9	106.0 ± 1.0	106.0 ± 1.1	104.5 ± 0.5	104.4 ± 0.5	104.1 ± 0.7
	Min1cc	91.9 ± 0.9	**90.2 ± 2.9**	**90.0 ± 2.9**	91.6 ± 1.0	**87.8 ± 4.2**	**87.7 ± 4.2**	85.4 ± 5.2	**80.2 ± 5.8**	**80.0 ± 5.8**
	CI	1.41 ± 0.13	**1.36 ± 0.14**	**1.36 ± 0.14**	1.16 ± 0.04	**1.11 ± 0.04**	**1.11 ± 0.04**	1.16 ± 0.07	**1.10 ± 0.06**	**1.10 ± 0.06**
	HI	11.0 ± 1.4	10.9 ± 1.4	10.9 ± 1.4	9.4 ± 0.6	**10.4 ± 1.1**	**10.4 ± 1.1**	8.5 ± 1.4	**10.6 ± 1.8**	**10.5 ± 1.8**
CTVin	V95%	98.9 ± 0.9	99.0 ± 0.6	98.9 ± 0.6	98.9 ± 0.5	99.0 ± 0.5	99.0 ± 0.5	99.1 ± 0.3	**98.7 ± 0.4**	**98.6 ± 0.4**
	D1cc	107.8 ± 1.2	**107.4 ± 1.0**	**107.3 ± 1.1**	106.1 ± 1.0	106.0 ± 1.0	106.0 ± 1.1	104.3 ± 0.4	104.3 ± 0.4	104.0 ± 0.6
	Min1cc	92.9 ± 1.0	92.8 ± 0.9	**92.7 ± 1.0**	92.5 ± 1.4	92.4 ± 1.5	92.4 ± 1.5	92.4 ± 1.1	**91.7** ± 0.8	**91.5** ± 0.9
	CI	1.75 ± 0.2	**1.69 ± 0.2**	**1.68 ± 0.2**	1.43 ± 0.1	**1.38 ± 0.1**	**1.37 ± 0.1**	1.43 ± 0.2	**1.37 ± 0.1**	**1.36 ± 0.1**
	HI	9.9 ± 1.5	**9.5 ± 1.4**	**9.5 ± 1.4**	8.8 ± 0.6	**8.6 ± 0.6**	**8.6 ± 0.6**	6.8 ± 0.7	**7.5 ± 0.8**	**7.4 ± 0.7**

Table 2 legend: Average DVH results for the OARs. The Plan and Sim columns indicate the planned and 4D simulated parameters, respectively. The units of D1cc and Mean are presented as percentages of the prescribed dose. Statistical significance between planned and simulated doses is represented by bolding ($p<0.05$) and between fractionations by an asterisk ($p<0.05$).

		3D-CRT			RA			E-VMAT	
		Plan	Sim		Plan	Sim		Plan	Sim	
			5fr	15fr		5fr	15fr		5fr	15fr
Lung R	V40%	12.4 ± 3.9	12.5 ± 4.0	12.5 ± 4.0	11.9 ± 1.5	11.8 ± 1.7	11.8 ± 1.7	10.4 ± 2.5	10.1 ± 2.7	10.1 ± 2.7
	Mean	13.6 ± 3.4	13.6 ± 3.6	13.5 ± 3.6	13.8 ± 1.2	13.8 ± 1.4	13.7 ± 1.4	13.0 ± 2.0	13.0 ± 2.2	13.0 ± 2.2
	D1cc	97.3 ± 2.4	96.6 ± 2.5	**96.5 ± 2.6**	93.9 ± 2.9	**92.6 ± 3.6**	**92.6 ± 3.6**	92.6 ± 3.9	**91.2 ± 4.7**	**91.1 ± 4.6**
Lung L	D1cc	1.7 ± 0.7	1.7 ± 0.7	1.7 ± 0.7	3.7 ± 2.1	**3.6 ± 2.1**	**3.6 ± 2.1**	4.0 ± 2.0	4.1 ± 1.9*	4.1 ± 1.9*
	Mean	0.4 ± 0.1	0.4 ± 0.1	0.4 ± 0.1	0.6 ± 0.1	0.6 ± 0.1*	0.6 ± 0.1*	1.1 ± 0.2	**1.2 ± 0.3**	**1.2 ± 0.3**
Heart	D1cc	7.6 ± 7.6	7.7 ± 7.3	7.7 ± 7.3	10.0 ± 5.9	10.2 ± 6.1	10.2 ± 6.1	7.6 ± 4.6	7.7 ± 4.0	7.7 ± 4.0
	Mean	1.2 ± 0.2	1.2 ± 0.2	1.2 ± 0.2	1.6 ± 0.3	1.6 ± 0.3	1.6 ± 0.3	2.0 ± 0.4	**2.2 ± 0.4**	**2.2 ± 0.4**
Breast L	D1cc	5.6 ± 4.1	**5.0 ± 3.1**	**5.0 ± 3.1**	27.1 ± 10.6	**24.9 ± 8.9**	**24.9 ± 8.9**	12.3 ± 4.2	**11.3 ± 3.4**	**11.3 ± 3.3**
	Mean	0.6 ± 0.2	**0.6 ± 0.2**	**0.6 ± 0.2**	2.1 ± 0.6	**2.0 ± 0.6**	**2.0 ± 0.6**	1.6 ± 0.4	**1.7 ± 0.4**	**1.7 ± 0.4**
Liver	D1cc	29.3 ± 31.6	34.9 ± 32.6	34.9 ± 32.6	24.2 ± 26.5	28.1 ± 24.7	28.1 ± 24.6	21.8 ± 25.2	26.1 ± 23.5	26.1 ± 23.5
Body	D1cc	108.6 ± 1.1	**107.9 ± 1.0**	**107.8 ± 1.1**	106.4 ± 0.8	**106.1 ± 0.9**	106.1 ± 1.0	104.8 ± 0.6	104.5 ± 0.5*	**104.2 ± 0.7***

Areas of underdose were observed inferior to the PTV, in the anterior and lateral chest wall region and between the PTV and sternum. Slight overdose was observed superior to the PTV, in the superior part of liver and in the middle lobe of the ipsilateral lung (Figure 2). However, statistically significant areas were found only for E-VMAT ($p<0.025$) and 5-fraction RA ($p<0.01$).

In terms of fractionation, no clinically significant differences were found between the 5 and 15-fraction dose distributions. The largest averaged difference between the simulated mean doses was less than 0.4% of the prescribed dose (Table 1 & 2). Statistical significance between fractionations was found only for three DVH parameters.

Discussion

There were only slight differences between the static and respiratory motion perturbed VMAT distributions. Slight decreases in PTV dose coverage and homogeneity were observed for arc techniques, but the CTV dose coverage was retained on average. No significant decreases were found for PTV or CTV coverage when using 3D-CRT technique, which is in agreement with the previous studies utilizing tangential techniques [8-10].

The PTV dose coverage was mainly compromised in areas with steep dose fall-off gradients, such as the medial PTV region. The E-VMAT plans had a steep dose gradient in the medial part of PTV due to avoiding the contralateral breast and thus the most notable dose decrease was observed in the medial region of the PTV. The decrease might be avoided by decreasing the dose gradient in this region, although this might result in increased dose to contralateral tissue. The RA planning did not result in a similar steep dose gradient in this region and the dose decrease in the medial parts of CTV was thus smaller in volume. However, dose to the contralateral breast was higher compared to E-VMAT.

The largest respiratory motion induced decrease in PTV dose coverage was found within the same patient regardless of the technique (~2% for 3D-CRT, 4.1 – 4.7% for RA and E-VMAT). This patient had the largest measured chest wall motion range (5.3 mm), whereas the average motion range was 2.4 mm in the included patients. A range of over 5 mm has been considered to have clinically significant impact in a study using the wedge technique [9]. Also AAPM Task Group 76 recommended using respiratory management for ranges over 5 mm [17].

Changes in HI of PTV indicated decreased homogeneity for VMAT plans. However, the decrease in CTV homogeneity was small for all techniques, even though the formula for HI is susceptible to changes in D2% and D98%, respectively. This suggests that respiratory motion increased dose heterogeneity in the areas of PTV margin. The PTV and CTV conformity increased consistently with respiratory motion for all patients. However, the changes in CI were small, although statistically significant.

On average, the DVH parameters determined for 5-fraction plans were equal to those determined for 15-fraction plans. For one patient, the perturbed 5-fraction 3D-CRT distribution retained the PTVin coverage goal while the corresponding 15-fraction distribution did not (difference of 0.7 percentage points (pp)). Similar effect was observed in the CTVin coverage of the same patient. In this study, ultra-hypofractionation resulted in longer beam-on times (136 s versus 83 s, for RA), which might be advantageous in terms of fraction specific dose averaging. A similar result was observed in an earlier study, where a smaller ratio between respiratory period and beam-on time lead to smaller deviation in dose distribution with the IMRT technique [11].

The most significant changes in OAR parameters were observed for maximum doses as the changes in mean dose were marginal. Dose to the ipsilateral lung decreased slightly in the chest wall region and increased slightly in the center of the lower lobe. Furthermore, large variation in liver maximum dose was observed. As the end-inspiration phase was used to create treatment plans, this variation was expected.

Some limitations exist. The included patients were initially treated for lung cancer and retrospectively selected for this study to investigate the effects of respiratory motion on the planned WBI dose distributions. However, as the patients' average chest wall motion range was similar to the breast cancer patients' respiratory motion range observed in previous studies, the present patient group was considered suitable for the study [8,9]. Furthermore, non-rigid fusions were used to transform and superimpose respiratory phase specific dose distributions to the end-inspiration phase. Inaccuracies in non-rigid fusions may generate uncertainty to simulated dose distributions and thus, exaggerate differences between planned and simulated distributions. To evaluate the quality of non-rigid fusion, all structures delineated to end-inspiration CT were deformed and transformed to other respiratory phases and quality of deformed structures was visually reviewed. Finally, it should be noted that other sources of error, such as tissue deformation [18], setup error [19] and variability in respiratory patterns [20,21], were not considered in this study.

The choice of fractionation did not impose clinically significant effects in the simulated dose distributions. The results suggest that ultra-hypofractionated VMAT and 3D-CRT treatments can be considered feasible for right-sided WBI under free-breathing conditions in terms of respiratory motion induced error.

Conclusion

Respiratory motion did not result in significant changes between planned and simulated dose distributions for WBI in this study population. Both 5 and 15-fraction approaches provided feasible results for VMAT and 3D-CRT under free-breathing conditions. The margins used were enough to maintain the CTVin dose coverage, although steep gradients should be avoided in areas close to the CTV.

List Of Abbreviations

3D-CRT: three-dimensional conformal radiation therapy; 4D-CT: four-dimensional computed tomography; AAA: analytical anisotropic algorithm; CBCT: cone-beam computed tomography; CI: conformity index; CP: control point; CTV: clinical target volume; DVH: dose-volume histogram; E-VMAT: Elekta VMAT; FB: free-breathing; HI: homogeneity index; IMRT: intensity-modulated radiation therapy; MLC: multi-leaf collimator; MU: monitor unit; OAR: organ-at-risk; PTV: planning target volume; RA: Rapid Arc; RPM: real-time position management; TPS: treatment planning system; VMAT: volumetric modulated arc therapy; WBI: whole-breast irradiation

Declarations

Ethics approval and consent to participate

The study protocol was approved by Central Finland Health Care District.

Consent for publication

Not applicable.

Availability of data and materials

The datasets generated and analyzed during the current study are not publicly available due to protection of individual patient privacy but are available from the corresponding author on reasonable request and with permission of Central Finland Health Care District.

Competing interests

The authors declare that they have no competing interests.

Funding

This research was funded by State research funding granted by the Finnish Ministry of Social Affairs and Health.

Author's Contributions

The study was conceptualized and designed by MM, TV, JS and TK. The data was collected and generated by MM and HH. Data processing tool development and analysis was conducted by MM and TV. The first draft of the manuscript was written by MM and all authors commented on the previous versions of the manuscript. All authors read and approved the final manuscript.

Acknowledgements

Thanks to Tuomas Selander (KUH) is for aiding with the statistical analysis, and to Aarno Kärnä (Hospital Nova) for technical assistance and intellectual discussions.

References

[1] START Trialists' Group, Bentzen SM, Agrawal RK, Aird EG, Barrett JM, Barrett-Lee PJ et al. The UK Standardisation of Breast Radiotherapy (START) Trial B of radiotherapy hypofractionation for treatment of early breast cancer: a randomised trial. Lancet 2008;371(9618):1098-107, https://doi.org/10.1016/S0140-6736(08)60348-7

[2] Brunt AM, Haviland JS, Wheatley DA, Sydenham MA, Alhasso A, Bloomfield DJ et al. Hypofractionated breast radiotherapy for 1 week versus 3 weeks (FAST-Forward): 5-year efficacy and late normal tissue effects results from a multicentre, non-inferiority, randomised, phase 3 trial. Lancet 2020;395(10237):1613-1626, https://doi.org/10.1016/s0140-6736(20)30932-6

[3] Rodin D, Tawk B, Mohamad O, Grover S, Moraes FY, Yap ML et al. Hypofractionated radiotherapy in the real-world setting: An international ESTRO-GIRO survey. Radiother Oncol 2021;157:32-39, https://doi.org/10.1016/j.radonc.2021.01.003

[4] Hunter D, Mauldon E, Anderson N. Cost-containment in hypofractionated radiation therapy: a literature review. J Med Radiat Sci 2018;65(2):148-157, https://doi.org/10.1002/jmrs.273

[5] Popescu CC, Olivotto IA, Beckham WA, Ansbacher W, Zavgorodni S, Shaffer R et al. Volumetric modulated arc therapy improves dosimetry and reduces treatment time compared to conventional intensity-modulated radiotherapy for locoregional radiotherapy of left-sided breast cancer and internal mammary nodes. Int J Radiat Oncol Biol Phys 2010;76(1):287-95, https://doi.org/10.1016/j.ijrobp.2009.05.038

[6] Bogue J, Wan J, Lavey RS, Parsai EI. Dosimetric comparison of VMAT with integrated skin flash to 3D field-in-field tangents for left breast irradiation. J Appl Clin Med Phys 2019;20(2):24-29, https://doi.org/10.1002/acm2.12527

[7] Virén T, Heikkilä J, Myllyoja K, Koskela K, Lahtinen T, Seppälä J. Tangential volumetric modulated arc therapy technique for left-sided breast cancer radiotherapy. Radiat Oncol 2015;10:79, https://doi.org/10.1186/s13014-015-0392-x

[8] Richter A, Sweeney R, Baier K, Flentje M, Guckenberger M. Effect of breathing motion in radiotherapy of breast cancer: 4D dose calculation and motion tracking via EPID. Strahlenther Onkol 2009;185(7):425-30, https://doi.org/10.1007/s00066-009-1980-1

[9] Jones S, Fitzgerald R, Owen R, Ramsay J. Quantifying intra- and inter-fractional motion in breast radiotherapy. J Med Radiat Sci 2015;62(1):40-6, https://doi.org/10.1002/jmrs.61

[10] Bedi C, Kron T, Willis D, Hubbard P, Milner A, Chua B. Comparison of radiotherapy treatment plans for left-sided breast cancer patients based on three- and four-dimensional computed tomography imaging. Clin Oncol 2011;23(9):601-7, https://doi.org/10.1016/j.clon.2011.04.004

[11] Ding C, Li X, Huq MS, Saw CB, Heron DE, Yue NJ. The effect of respiratory cycle and radiation beam-on timing on the dose distribution of free-breathing breast treatment using dynamic IMRT. Med Phys 2007;34(9):3500-9, https://doi.org/10.1118/1.2760308

[12] Chung JH, Chun M, Kim JI, Park JM, Shin KH. Three-dimensional versus four-dimensional dose calculation for breast intensity-modulated radiation therapy. Br J Radiol 2020;93(1110):20200047, https://doi.org/10.1259/bjr.20200047

[13] Offersen BV, Boersma LJ, Kirkove C, Hol S, Aznar MC, Biete Sola A et al. ESTRO consensus guideline on target volume delineation for elective radiation therapy of early stage breast cancer. Radiother Oncol 2015;114(1):3-10, https://doi.org/10.1016/j.radonc.2014.11.030

[14] Nicolini G, Fogliata A, Clivio A, Vanetti E, Cozzi L. Planning strategies in volumetric modulated arc therapy for breast. Med Phys 2011;38(7):4025-31, https://doi.org/10.1118/1.3598442

[15] Heikkilä J, Virsunen H, Voutilainen L, Vuolukka K, Nevantaus A, Haatanen M et al. PO-1104 Implementing an automated target delineation service in multi-institutional environment in Finland, https://www.thegreenjournal.com/article/S0167-8140(19)31524-5/fulltext; 2019 [accessed 9 July 2021]

[16] Benjamini Y, Hochberg Y. Controlling the false discovery rate: a practical and powerful approach to multiple hypothesis testing. J Roy Stat Soc B Met 1995;57(1):289-300, https://doi.org/10.1111/j.2517-6161.1995.tb02031.x

[17] Seppälä J, Vuolukka K, Virén T, Heikkilä J, Honkanen JTJ, Pandey A et al. Breast deformation during the course of radiotherapy: The need for an additional outer margin. Phys Med 2019;65:1-5, https://doi.org/10.1016/j.ejmp.2019.07.021

[18] Batumalai V, Holloway L, Delaney GP. A review of setup error in supine breast radiotherapy using cone-beam computed tomography. Med Dosim, 2016;41(3):225-9, https://doi.org/10.1016/j.meddos.2016.05.001

[19] Persson GF, Nygaard DE, Olsen M, Juhler-Nøttrup T, Pedersen AN, Specht L et al. Can audio coached 4D CT emulate free breathing during the treatment course? Acta Oncol 2008;47(7):1397-405, https://doi.org/10.1080/02841860802256442

[20] Jensen CA, Acosta Roa AM, Lund JÅ, Frengen J. Intrafractional baseline drift during free breathing breast cancer radiation therapy. Acta Oncol 2017;56(6):867-873, https://doi.org/10.1080/0284186x.2017.1288924

[21] Keall PJ, Mageras GS, Balter JM, Emery RS, Forster KM, Jiang SB et al. The Management of Respiratory Motion in Radiation Oncology of AAPM Task Group 76. Med Phys 2006;33(10):3874-900, https://doi.org/10.1118/1.2349696

Figures

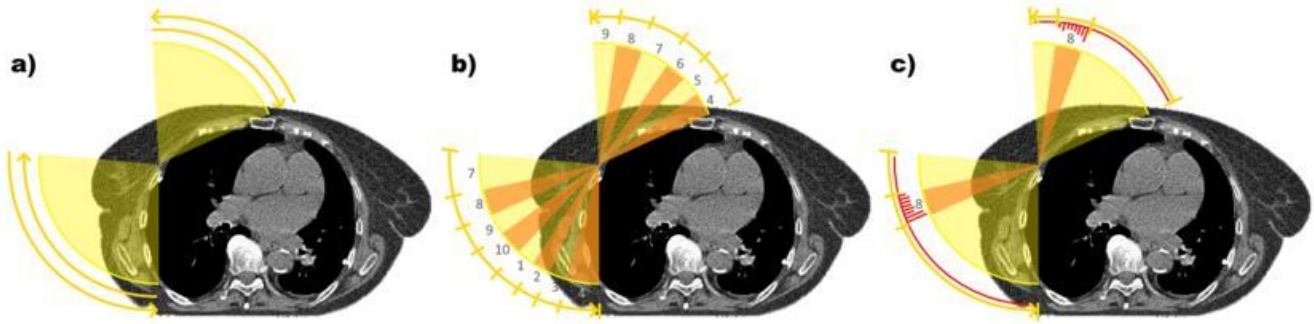

Figure 1

The original arc plan with four arcs (a) was divided into respiratory phase-specific subplans (b), where the starting respiratory phases 4 and 7 were randomly determined for the anterior and posterior arcs. The subplan targeting the eighth respiratory phase (c) only contained irradiation coinciding with that respiratory phase. The MUs delivered in the phase-specific subplan (c) are indicated with bars. Dose rate is zeroed between CPs not coinciding with the eighth respiratory phase.

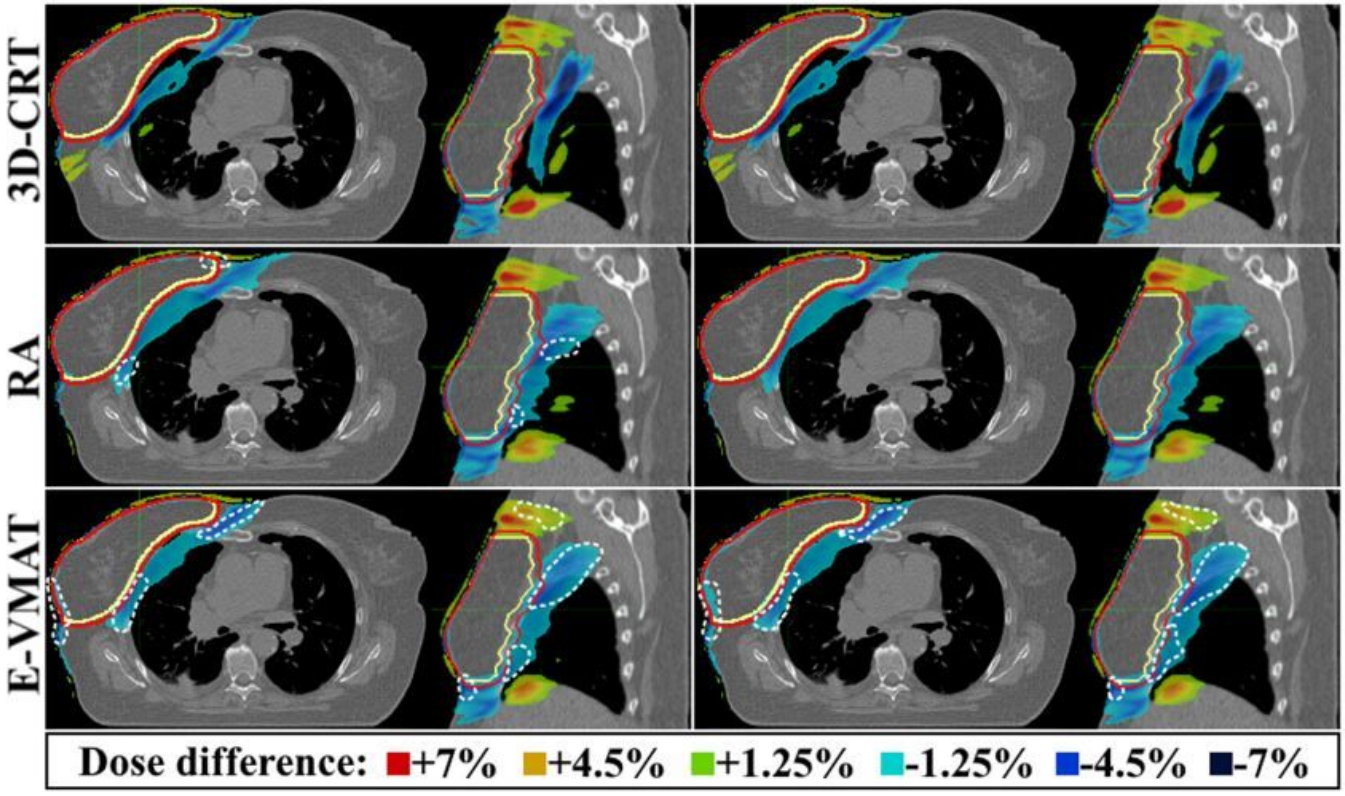

Figure 2

Axial and sagittal views of the differential dose distributions. The colored areas indicate over-/underdose in the respiratory motion perturbed distribution compared to the original as percentages of the prescribed dose. Statistically significant areas are encircled with dashed lines ($p<0.01$ for RA and $p<0.025$ for E-VMAT). The CTV and PTV contours are illustrated in yellow and red, respectively.

Supplementary Files

This is a list of supplementary files associated with this preprint. Click to download.

- axialdeformeddifferentialdoseEVMAT15.gif
- axialdeformeddifferentialdoseRA5.gif
- axialdeformeddifferentialdoseRA15.gif
- supplementaryanimation6caption.txt
- supplementaryanimation1caption.txt
- supplementaryanimation2caption.txt
- supplementaryanimation3caption.txt
- supplementaryanimation4caption.txt
- supplementaryanimation5caption.txt
- axialdeformeddifferentialdose3DCRT5.gif
- axialdeformeddifferentialdose3DCRT15.gif
- axialdeformeddifferentialdoseEVMAT5.gif